

Phyto-mediated silver nanoparticles via *Mellisa officinalis* aqueous and methanolic extracts: synthesis, characterization and biological properties

Fatemeh Dehghan Nayeri (✉ fatemeh_dn@yahoo.com)

Imam Khomeini International University

Sudabeh Mafakheri

Department of Horticulture Science, Faculty of Agricultural and Natural Sciences, Imam Khomeini International University (IKIU), Qazvin, Islamic Republic of Iran

Maryam Mirhosseini

Department of Agricultural Biotechnology, Faculty of Agricultural and Natural Sciences, Imam Khomeini International University (IKIU), Qazvin, Islamic Republic of Iran.

Research

Keywords: Bio-reducing agent, Characterization, Green synthesis, Plant extract, Silver nanoparticles

Posted Date: May 10th, 2020

DOI: <https://doi.org/10.21203/rs.3.rs-24102/v1>

License:  This work is licensed under a Creative Commons Attribution 4.0 International License.

[Read Full License](#)

Abstract

The aim of the study was to examine the influence of extraction method on the size, shape and morphology of synthesized silver nanoparticles (AgNPs). Silver nanoparticles were prepared by the aqueous and methanolic extracts of lemon balm. The properties of obtained nanoparticles were characterized by UV-Vis, SEM, XRD and FTIR techniques. The UV-Vis spectroscopy confirmed the formation of AgNPs by observing a distinct surface Plasmon resonance band around 450 nm. SEM images showed different shape, size and morphology of AgNPs using two different extracts types. AgNPs derived from the aqueous extract were rod-shaped with a diameter of 19 to 40 nm whereas spherical particles were synthesized by the methanolic extract found smaller with size distribution ranging from 13 to 35 nm. The XRD pattern indicated that AgNPs formed by the reduction of Ag⁺ ions using methanolic extract of *M. officinalis* were crystal-like in nature. The functional groups of *M. officinalis* methanolic extract involved in synthesis and stabilization of AgNPs were investigated by FTIR. In addition, AgNPs-containing methanolic extract showed higher antioxidant activity. These particles exhibited remarkable antimicrobial activity against gram positive and negative bacteria and a fungus. The nanoparticles produced by the methanolic extract of the lemon balm showed antioxidant and antimicrobial activity. The production of silver nanoparticles using plant extract is rapid, low cost and eco-friendly. Therefore, green chemistry is a good alternative to industrial production of nanoparticles. Silver nanoparticles can be used as an antiseptic to sterilize the surrounding area and the hospital wastes.

1. Introduction

Utilization of biocompatible and ecofriendly processes for the production of nanoparticles is of great importance in current nanotechnology research [1]. Nanomaterials have been synthesized by different methods including hard template [2], bacteria [3], fungi [4] and plants [5]. During the synthesis of metallic nanoparticles by chemical methods toxic compounds are often produced which remains adsorbed on the particle surface and has adverse effects on human health. However, the green synthesis is based on non-toxic and environmentally friendly ingredients. It is cost-effective, low energy consumption, less complex and less time-consuming process [6]. Among all types of nanoparticles, silver nanoparticles (AgNPs) have been used for a variety of applications in everyday life [7]. AgNPs have more application in the medical field as antimicrobials and sterilizers [8]. The antimicrobial property of silver nanoparticles is well known and mediated by the released silver cations from silver nitrate (AgNO₃) [9].

Because of advantages of biological processes in synthesis of nanoparticles [10], various plant resources have been explored by researchers to synthesize nanoparticles such as *Coriandrum sativum* [11], *Berberis vulgaris* [12], *Cassia toral* [13], *Moringa oleifera* [14], *Malva sylvestris* [15], *Gossypium hirsutum* [16], *Gelidium amansii* [17], *Aloe vera* [18] and *Melissa officinalis* [19]. *Melissa officinalis* L. is a perennial and medicinal herb from the Labiatae (Lamiaceae) family. Because of its lemon-like fragrance known as lemon balm [20]. Different organic compounds present in lemon balm extract including protein, essential oils, flavonoids, rosmarinic, caffeic and gallic acids and phenolic contents are responsible for bio-

reduction of Ag⁺ ions [19, 21]. *M. officinalis* as a valuable source of natural antioxidants has strong antimicrobial activity [22, 23]. In the present study, silver nanoparticles (AgNPs) were synthesized using aqueous and methanolic extracts of *Melissa officinalis*. Silver nitrate was used as a precursor and *M. officinalis* extracts as reducing and stabilizing agents. To investigate the influence of extraction method on the size, shape and morphology of synthesized AgNPs, aqueous and methanolic extracts of lemon balm were examined. To survey the effect of extract concentration on the rate of nanoparticle synthesis, the AgNPs were prepared using various concentrations of aqueous (7, 10, 15 and 20 ml) and methanolic (0.1, 0.5, 1 and 5 mg) extracts of lemon balm. The properties of obtained nanoparticles were characterized by ultraviolet-visible spectroscopy (UV-Vis), Scanning Electron Microscope (SEM), X-Ray Diffraction (XRD) and Fourier Transform Infrared (FTIR) techniques. The antioxidant ability of the AgNPs was assessed using DPPH (2,2-diphenyl-1-picrylhydrazyl) scavenging as well. Moreover, the bactericidal and fungicidal effects of AgNPs on *Bacillus subtilis*, *Staphylococcus aureus*, *Escherichia coli* and *Saccharomyces cerevisiae* were confirmed.

2. Materials And Methods

2.1. Plant extraction

2.1.1. Aqueous extract

The aerial parts of *Melissa officinalis* were washed with distilled water and shade dried for 7 days at room temperature. The dried plants were ground into a fine powder. For preparation of the aqueous extract 150 ml of sterile distilled water was added to 6 gr of powdered samples and boiled for 10 min. The suspension was left for 3 h and then filtered through Whatman No. 1 filter paper. The samples were centrifuged at a high speed (20000 rpm) for 15 min and kept at 4 °C until further analysis.

2.1.2. Methanolic extract

About 6 gr of powdered samples was uniformly packed into a thimble and placed in the Soxhlet extractor. It was exhaustible extracted with methanol for the period the solvent in siphon tube of extractor becomes colorless. The extracts were filtered using filter paper and the solvent evaporated from the extract in a rotary evaporator to have a syrupy consistency. The extract was stored at 4 °C for further experiments.

2.2. Biosynthesis of silver nanoparticles

The procedure for the preparation of silver nanoparticles has been adopted from Savithramma *et al.* [24] with slight modifications. 1 mM AgNO₃ (silver nitrate) solution was prepared and stored in amber colored bottle. 50 ml of AgNO₃ solution (1 mM) was added into 5 ml of lemon balm extracts with constant stirring at room temperature until the color change was observed. The color change of the solution is a sign for the formation of silver nanoparticles. The extract content was then centrifuged at 14000 rpm for 30 min. To monitor the reduction of Ag⁺ ions and the formation of AgNPs ultraviolet-visible spectroscopy was used.

2.3. Characterization of synthesized silver nanoparticles

The biosynthesized AgNPs were analyzed using UVD-3200 spectrophotometer. Their spectral analysis was done in the range of 300 to 800 nm. The size and shape of AgNPs were determined by SEM using MIRA-3 SEM machine. The lyophilized powdered sample was used for XRD and FTIR (Bruker Tensor 27) spectroscopy analysis. The XRD patterns were recorded using Bruker D8 Advance X-ray diffractometer with a Cu K_α radiation. FTIR was used to characterize the nanoparticles using the lyophilized samples by potassium bromide pellet technique in the range of 500 to 4000 cm⁻¹.

2.4. DPPH free radical scavenging assay

Antioxidant activity of AgNPs was quantitatively studied using DPPH method [25]. Briefly, 150 μl of 1 mM nanoparticle solution and ascorbic acid (positive control) were taken separately and mixed with 2850 μl of a methanolic solution of DPPH. The reaction mixture was shaken and kept in a dark place for 24 h. After incubation, the absorbance of the samples (reduction of DPPH radical) was measured by UV–Vis spectrophotometer at 517 nm against methanol as blank. The methanolic solution of DPPH without the sample served as control. The DPPH free radical scavenging activity (percentage of inhibition) was calculated using the following formula:

$$\text{Inhibition (\%)} = \frac{A_{\text{control}} - A_{\text{sample}}}{A_{\text{control}}} \times 100$$

2.5. Antimicrobial assays of the biosynthesized AgNPs

The antimicrobial efficacy of synthesized silver nanoparticles was observed against *Bacillus subtilis*, *Staphylococcus aureus*, *Escherichia coli* and *Saccharomyces cerevisiae*. This property was assayed by both the standard Kirby–Bauer disc diffusion [26] and agar well diffusion methods [27]. Briefly, the agar plates were inoculated with 100 μl of 1 × 10⁶ bacterial and fungal suspension using spread-plating. After drying the plates, filter paper discs of 6-mm diameter were soaked in 30 and 40 μl of biosynthesized AgNPs solution (1 mM), plant extract and distilled water as control and placed on LB agar plates followed by incubation at 37 °C (Bacteria) and 28 °C (*Saccharomyces cerevisiae*) for 24 h. Susceptibility of organisms were determined by measuring diameter of inhibition zone (mm) with a ruler.

For agar well diffusion test, the agar plates were inoculated with 100 μl of 1 × 10⁶ bacterial and fungal suspension using spread-plating. After drying the plates, wells of 6-mm diameter were punched into the agar medium, aseptically filled with 20, 30 and 40 μl of biosynthesized nanoparticle solution (1 mM nanoparticle) and plant extract and allowed to diffuse for 2 h at room temperature. The plates were subsequently incubated at 37 °C (Bacteria) and 28 °C (*Saccharomyces cerevisiae*) for 24 h. The antimicrobial activity was analyzed by measuring the diameter of inhibition zone (mm) around the wells.

3. Results And Discussion

3.1. Color change

The reduction of silver ions into silver nanoparticles can be followed by color change. The fresh extract of *M. officinalis* was pale yellow in color. After addition of AgNO_3 and stirring at room temperature, the solution color changed into pale pink (within 30 minutes for aqueous extract) and light red (within 15 minutes for methanolic extract). The emulsion turned dark brown after 24 and 36 h for methanolic and aqueous extracts respectively.

In this study different volumes of aqueous extract (7, 10, 15 and 20 ml) was used. Change in color in the aqueous extract of lemon balm during chemical reaction of biosynthesis of silver nanoparticles was initiated within 30 minutes. At first, color change was occurred in the sample of 7-ml aqueous extract. This process was completed in this sample earlier than the other volumes of aqueous extract (Fig. 1).

The methanolic extract was used at 0.1, 0.5, 1, and 5 mg /50 ml of the reaction volume. The concentration of 0.1 mg showed no color variation and silver nanoparticles were not produced at this concentration. Change in color in the methanolic extract of lemon balm was initiated within 15 minutes. Our obtained results showed that the speed of chemical reaction was increased by increasing the concentration of methanolic extract. So in the used concentrations, 5 milligrams responded best (Fig. 2). As the concentration of lemon balm extract varies, the nanoparticle synthesis also varies.

The size of colloidal particles is between 1 to 1000 nm. The formation of colloidal solutions from the reduction of silver ions occurs in two steps (nucleation and growth) (Fig. 3). According to the researchers, metal precursor, reducing and stabilizing agents are major components in the formation of metal nanoparticles [28, 29]. In the biological process plant metabolites such as sugars, proteins, terpenoids, polyphenols, alkaloids, flavonoids and phenolic acids are responsible for the reduction and stabilization of nanoparticles [30]. It has been reported that the OH groups present in flavonoids play a role in the reduction of silver ions to AgNPs [31]. Based on the results obtained till this step, two experiments (DPPH and SEM) were performed only on the samples of 7-ml aqueous and 5-mg /50 ml methanolic extracts.

3.2. Antioxidant capacity (DPPH radical scavenging assay)

The DPPH free radical scavenging assay was determined by measuring the ability of plant extracts to capture the stable radical 2,2-diphenyl-1-picrylhydrazyl (DPPH) [25, 32]. The primary DPPH solution is violet which changes to yellow. The violet color disappears as soon as adding synthesized silver nanoparticles because of the presence of antioxidant in the medium. However, the process of yellowing may slow down and the target substance exhibits poor antioxidant activity or no color change. The inhibitory concentration of the material is investigated based on the absorbance of 2,2-diphenyl-1-picrylhydrazyl radiation at a wavelength of 517 nm. The antioxidant effect of lemon balm extracts and silver nanoparticles showed that the methanolic extract had the highest antioxidant activity among the tested specimens. Subsequently, the aqueous extract and the nanoparticle showed antioxidant activity.

The color change rate in the methanolic extract was also higher than that of the aqueous and silver nanoparticles (Fig. 4).

Several studies with enhanced DPPH scavenging activity by AgNPs from plant extracts have been investigated [33–35]. The production of iron nanoparticles using aqueous extract of 26 tree species and antioxidant properties of their extract have been reported. These researchers interestingly found dried leaves produce extracts with higher antioxidant capacities than non-dried leaves. This is probably due to evaporation of water present in the leaves and increasing of antioxidants concentration [36].

3.3. Scanning electron microscope

To determine the morphological characters of silver nanoparticles synthesized by lemon balm extracts, scanning electron microscope (SEM) was used. The SEM images showed rod-shaped nanoparticles formed with diameter in the range of 19–40 nm from the aqueous extract. Also the nanoparticles derived from the methanolic extract were spherical with diameter of 13–35 nm (Fig. 5).

It has been reported that the nanoparticles deformation as different shapes and diameters is the result of altering the plant extract and/or the reaction conditions depending on the application [30]. The surface areas and the shapes of nanoparticles affect on their antimicrobial activity [37, 38] due to different effective surface areas and active facets [39, 40]. It was suggested that *Melissa officinalis* scavenged DPPH radical in a concentration-dependent manner [21] that is in agreement with the result of our study. DPPH assay revealed the sample of 5-mg /50 ml methanolic extract had the highest antioxidant activity compared to the 7-ml aqueous extract.

Based on the SEM results, the particles produced by methanolic extract were spherical and smaller in size in comparison to the rod-shaped particles derived from the aqueous extract. Therefore, further experiments were conducted using the methanolic sample.

3.4. Ultraviolet-visible spectroscopy

Color change from yellow to brownish-red and dark brown is the first sign of nanoparticle production and is due to excitation of the surface Plasmon resonance [41]. The biosynthesis of nanoparticle should be confirmed via physical methods like UV-Vis spectrophotometer, SEM, XRD and FTIR [34, 42].

The biosynthesis of SNPs and the reduction of Ag^+ ions to Ag atoms were recorded by UV-Vis spectroscopy. The reaction was conducted for a duration of 2 h. The UV-Vis absorption spectra of colloidal solutions of SNPs using *M. officinalis* methanolic extract had absorbance near 450 nm. The broadening peak is a sign of the poly-dispersed particles formation (Fig. 6). Hafez *et al.* (2017) produced AgNPs that showed UV-Vis absorbance at 425 nm [43] and Keshari *et al.* (2018) reported the absorption band of AgNPs at 442 nm [44]. Also, the absorption of the SNPs was observed near 430 nm in the UV-Vis spectrum [45]. The absorbance wavelength depends on the concentration of plant extract [46, 47], different times [47, 48], fresh and freeze-dried samples [14] and particle size [40, 49].

3.5. Antimicrobial property of AgNPs

The antimicrobial effect of spherical silver nanoparticles was investigated by disc diffusion and agar well diffusion methods. Based on our findings, green synthesis of the silver nanoparticles using this herb showed an effective antimicrobial activity against *B. subtilis* and *S. aureus* gram-positive and *E. coli* gram-negative bacteria and *S. cerevisiae* (Figs. 7 and 8).

The inhibition zone of bacteria and fungus was measured in millimeter. In disc method the size of inhibition zone for *B. subtilis*, *S. aureus*, *E. coli* and *S. cerevisiae* was measured 5.7, 5.6, 7 and 4 respectively (Fig. 7). The size of inhibition zone of *B. subtilis*, *S. aureus*, *E. coli* and *S. cerevisiae* was calculated in agar well diffusion method 10, 10, 11.3 and 9.25 mm, respectively (Fig. 8). In both methods gram-negative bacterium of *E. coli* showed the highest sensitivity to the silver nanoparticles. The bactericidal effect of silver nanoparticles is size and shape dependent. Smaller particles have higher percentage of the surface area than bigger particles [50]

In a previous study, antibacterial property of SNPs derived from aqueous extract of lemon balm leaves against *S. aureus* and *E. coli* was confirmed [19]. Our results elucidated that silver nanoparticles from methanolic extract of lemon balm inhibited bacterial and fungal growth. As expected, increasing the amount of nanoparticles showed more deterioration and increased the growth halo. In the present study it was revealed that both gram-negative and gram-positive bacterial strains were more susceptible to AgNPs than the fungus strain. Although AgNPs exert antifungal activity due to interaction with the fungal cell wall and membrane which leads to cell death through disruption of cell membrane structure [51]. These differences in bactericidal and fungicidal effects of the AgNPs are due to the differences in organization of the bacterial and fungal cells. The bacteria are evolutionarily prokaryotic types and are less complex. Therefore, they are unable to fight the toxic effects of AgNPs as effectively as the eukaryotic fungi. The eukaryotic organisms have superior detoxification system that makes them resistance to higher concentrations of AgNPs [52].

Attack on the surface of the bacteria membrane through interaction with sulfur-containing proteins [53], disruption of cell permeability and respiration, form the pits on the cell surface and induce the proton leakage as a consequence of cell death [54, 55], inhibition of respiratory enzymes of bacterial cells by combining with the group thiol [50] as well as cell retention of DNA replication and preventing reproduction [56, 57] are among the reasons given for the antimicrobial properties of silver nanoparticles. A possible mechanism was depicted for AgNPs formation and their antimicrobial activities (Fig. 9).

3.6. X-ray diffraction analysis

X-ray diffraction (XRD) is one of the most widely used techniques to characterize the structural properties of NPs. To gain structural information, the resulting diffraction pattern obtained from the penetration of X-rays into the nanomaterials is compared with standards [58, 59]. Figure 10 shows the XRD pattern of the synthesized AgNPs using the methanolic extract of lemon balm. The AgNPs diffractogram displayed

several sharp intense peaks at 2 theta angles, which indicated towards the crystallinity of the AgNPs and confirmed the formation of the silver nanoparticles. Four distinct reflections at 37.5° (111), 44.37° (200), 64.56° (220) and 76.58° (311) evidently indicated the formation of the face-centered cubic structure of the AgNPs in the prepared sample (Fig. 10).

The XRD outline accordingly obviously displayed that the silver nanoparticles formed by the reduction of Ag⁺ ions by *Melissa officinalis* extract are crystal-like in nature. This result is consistent with XRD analysis of Shaik *et al.* (2018) [46]. Additional peaks at 32.25° and 54.62° were observed on the preparation of AgNPs using *M. officinalis* methanolic extract (Fig. 10). These peaks are attributed to the existence of some bioorganic compounds in *M. officinalis* leaf broth [60] or related to unreduced and remained AgNO₃ in the sample [61]. It has been suggested that magnesium chlorophyll is the center of X-ray diffraction in the bioorganic crystalline phase [62].

3.7. Fourier transform infrared spectroscopy

Here, Fourier transform infrared spectroscopy (FTIR) was used to analyze the chemical composition of lemon balm responsible for reduction of Ag ions (Fig. 11). FTIR is useful for characterizing the surface chemistry. Using this technique organic functional groups (COO⁻, OH, ...) attached to the Ag and other chemical residues surface are detected.

The methanolic extract of aerial parts of lemon balm displayed a number of absorption peaks, reflecting its complex nature. The results of FTIR analysis showed different stretches of bonds shown at different peaks including 3446.51 cm⁻¹ could be assigned to O-H stretch, H-bonded corresponded to alcohols and phenols, 2357.56 cm⁻¹ assigned for single aldehyde, 1151.92 cm⁻¹ indicates the fingerprint region of C-O stretching, 674.99 cm⁻¹ could be attributed to the presence of C-H bend alkynes and 674.99 cm⁻¹ and 599.95 cm⁻¹ correspond to halo compound. Figure 11 shows the peaks near 3000 cm⁻¹ assigned to O-H stretching and aldehydic C-H stretching. The absorption peaks between 1500 to 2000 cm⁻¹ can be attributed to the presence of C-O stretching in carboxyl coupled to the amide linkage in amide I which is characteristic of the presence of protein and enzymes in the supernatant and confirms the extracellular formation of AgNPs [34, 63–67]. Consequently, the occurrence of these peaks in the FTIR spectrum evidently indicates the dual role of the *M. officinalis* extract, both as a green reducing and stabilizing agents.

Interactions between metabolites in the extract and metal ions cause the bioreduction of metal salts and synthesis of nanoparticles. The functional groups in the plant extract act as reducing, capping, and stabilizing agents [58, 68]. Negatively charged (COO⁻) and polar (OH and CO) groups presented in the plant extract attach on the Ag surface with high tendency and contribute in both reduction and stabilization of AgNPs [69].

4. Conclusion

Here, biosynthesis of silver nanoparticles using lemon balm extracts and their antibacterial, antifungal and antioxidant activities were studied. According to the results, the nanoparticles produced by the methanolic extract of the lemon balm showed antioxidant and antimicrobial activities. The production of AgNPs using plant extract is rapid, eco-friendly and low-cost. In this method, there is no need to use expensive raw and hazardous materials [70]. Therefore, green chemistry is a good alternative to industrial production of nanoparticles. Due to the antimicrobial properties of these particles on the tested materials, they can be used as an antiseptic to sterilize the surrounding area and the hospital wastes. Also, antioxidant properties of nanoparticles can be exploited in food industry. The syntheses of spherical and rod-shaped silver nanoparticles with different dimensions were observed using *M. officinalis* methanolic and aqueous extracts respectively. Therefore, deformation of resulting nanoparticles indicated that by changing the plant extract type and the reaction conditions, nanoparticles with different shapes and diameters formed.

Abbreviations

AgNO₃

Silver nitrate

AgNPs

Silver nanoparticles

DPPH

2,2-diphenyl-1-picrylhydrazyl

FTIR

Fourier Transform Infrared

M. officinalis

Melissa officinalis

SEM

Scanning Electron Microscope

SNPs

Silver nanoparticles

XRD

X-Ray Diffraction

UV

Ultraviolet

UV-Vis

Ultraviolet-visible spectroscopy

Declarations

Ethics approval, consent to participate

Not applicable.

Consent for publication

All authors have read and approved to submit it to *Bioresources and Bioprocessing*.

Availability of data and materials

All data are available.

Competing interests

The authors declare that they have no competing interests.

Funding

This work was supported by the Imam Khomeini International University [grant number 11590].

Author's Contributions

F.D.N designed the experiment, analyzed and interpreted the data and wrote the main manuscript text, M.M performed experiments, collected the data and prepared figures and S.M. helped in performing experiments and writing the manuscript text. All the authors read and approved the final manuscript.

Acknowledgment

This work was done in Agricultural Biotechnology Department of Imam Khomeini International University. The authors appreciate all staffs on their good collaborations.

References

1. Subbaiya, R.;Shiyamala, M.;Revathi, K.;Pushpalatha, R.; Selvam, M. M. Biological synthesis of silver nanoparticles from Nerium oleander and its antibacterial and antioxidant property. *Int. J. Curr. Microbiol. App. Sci* 2014, 3, 83–87.
2. Suganthy, N.;Ramkumar, V. S.;Pugazhendhi, A.;Benelli, G.; Archunan, G. Biogenic synthesis of gold nanoparticles from Terminalia arjuna bark extract: assessment of safety aspects and neuroprotective potential via antioxidant, anticholinesterase, and antiamyloidogenic effects. *Environmental Science and Pollution Research* 2017, 1–16.
3. Deyev, S.;Proshkina, G.;Ryabova, A.;Tavanti, F.;Menzianni, M. C.;Eidelshtein, G.;Avishai, G.; Kotlyar, A. Synthesis, Characterization, and Selective Delivery of DARPIn–Gold Nanoparticle Conjugates to Cancer Cells. *Bioconjugate chemistry* 2017, 28, 2569–2574.
4. Khutale, G. V.; Casey, A. Synthesis and characterization of a multifunctional gold-doxorubicin nanoparticle system for pH triggered intracellular anticancer drug release. *European Journal of Pharmaceutics and Biopharmaceutics* 2017, 119, 372–380.

5. Kumar, V. K. R.; Gopidas, K. R. Synthesis and Characterization of Gold-Nanoparticle-Cored Dendrimers Stabilized by Metal–Carbon Bonds. *Chemistry–An Asian Journal* 2010, 5, 887–896.
6. Tagad, C. K.; Dugasani, S. R.; Aiyer, R.; Park, S.; Kulkarni, A.; Sabharwal, S. Green synthesis of silver nanoparticles and their application for the development of optical fiber based hydrogen peroxide sensor. *Sensors and Actuators B: Chemical* 2013, 183, 144–149.
7. Echegoyen, Y.; Nerín, C. Nanoparticle release from nano-silver antimicrobial food containers. *Food and Chemical Toxicology* 2013, 62, 16–22.
8. Rai, M.; Yadav, A.; Gade, A. Silver nanoparticles as a new generation of antimicrobials. *Biotechnology advances* 2009, 27, 76–83.
9. Hachicho, N.; Hoffmann, P.; Ahlert, K.; Heipieper, H. J. Effect of silver nanoparticles and silver ions on growth and adaptive response mechanisms of *Pseudomonas putida* mt-2. *FEMS microbiology letters* 2014, 355, 71–77.
10. Prasad, R. Synthesis of silver nanoparticles in photosynthetic plants. *Journal of Nanoparticles* 2014, 2014.
11. Ashraf, A.; Zafar, S.; Zahid, K.; Shah, M. S.; Al-Ghanim, K. A.; Al-Misned, F.; Mahboob, S. Synthesis, characterization, and antibacterial potential of silver nanoparticles synthesized from *Coriandrum sativum* L. *Journal of infection and public health* 2018.
12. Behravan, M.; Panahi, A. H.; Naghizadeh, A.; Ziaee, M.; Mahdavi, R.; Mirzapour, A. Facile green synthesis of silver nanoparticles using *Berberis vulgaris* leaf and root aqueous extract and its antibacterial activity. *International journal of biological macromolecules* 2019, 124, 148–154.
13. Shaikh, R.; Zainuddin Syed, I.; Bhende, P. Green synthesis of silver nanoparticles using root extracts of *Cassia toral* L. and its antimicrobial activities. *Asian Journal of Green Chemistry* 2019, 3, 70–81.
14. Moodley, J. S.; Krishna, S. B. N.; Pillay, K.; Govender, P. Green synthesis of silver nanoparticles from *Moringa oleifera* leaf extracts and its antimicrobial potential. *Advances in Natural Sciences: Nanoscience and Nanotechnology* 2018, 9, 015011.
15. Esfanddarani, H. M.; Kajani, A. A.; Bordbar, A.-K. Green synthesis of silver nanoparticles using flower extract of *Malva sylvestris* and investigation of their antibacterial activity. *IET nanobiotechnology* 2017, 12, 412–416.
16. Vanti, G. L.; Nargund, V. B.; Vanarchi, R.; Kurjogi, M.; Mulla, S. I.; Tubaki, S.; Patil, R. R. Synthesis of *Gossypium hirsutum*-derived silver nanoparticles and their antibacterial efficacy against plant pathogens. *Applied Organometallic Chemistry* 2019, 33, e4630.
17. Pugazhendhi, A.; Prabakar, D.; Jacob, J. M.; Karuppusamy, I.; Saratale, R. G. Synthesis and characterization of silver nanoparticles using *Gelidium amansii* and its antimicrobial property against various pathogenic bacteria. *Microbial pathogenesis* 2018, 114, 41–45.
18. Chandran, S. P.; Chaudhary, M.; Pasricha, R.; Ahmad, A.; Sastry, M. Synthesis of gold nanotriangles and silver nanoparticles using *Aloevera* plant extract. *Biotechnology progress* 2006, 22, 577–583.
19. de Jesús Ruíz-Baltazar, Á.; Reyes-López, S. Y.; Larrañaga, D.; Estévez, M.; Pérez, R. Green synthesis of silver nanoparticles using a *Melissa officinalis* leaf extract with antibacterial properties. *Results in*

Physics 2017, 7, 2639–2643.

20. Abdel-Naime, W. A.; Fahim, J. R.; Fouad, M. A.; Kamel, M. S. Botanical studies of the leaf of *Melissa officinalis* L., Family: Labiatae, cultivated in Egypt. *Journal of Pharmacognosy and Phytochemistry* 2016, 5, 98.
21. Kamdem, J. P.; Adeniran, A.; Boligon, A. A.; Klimaczewski, C. V.; Elekofehinti, O. O.; Hassan, W.; Ibrahim, M.; Waczuk, E. P.; Meinerz, D. F.; Athayde, M. L. Antioxidant activity, genotoxicity and cytotoxicity evaluation of lemon balm (*Melissa officinalis* L.) ethanolic extract: Its potential role in neuroprotection. *Industrial Crops and Products* 2013, 51, 26–34.
22. Kittler, J.; Krüger, H.; Ulrich, D.; Zeiger, B.; Schütze, W.; Böttcher, C.; Krähmer, A.; Gudi, G.; Kästner, U.; Heuberger, H. Content and composition of essential oil and content of rosmarinic acid in lemon balm and balm genotypes (*Melissa officinalis*). *Genetic Resources and Crop Evolution* 2018, 65, 1517–1527.
23. Abdellatif, F.; Boudjella, H.; Zitouni, A.; Hassani, A. Chemical composition and antimicrobial activity of the essential oil from leaves of Algerian *Melissa officinalis* L. *EXCLI journal* 2014, 13, 772.
24. Savithramma, N.; Lingarao, M.; Basha, S. Antifungal efficacy of silver nanoparticles synthesized from the medicinal plants. *Der Pharma Chemica* 2011, 3, 364–372.
25. Thaipong, K.; Boonprakob, U.; Crosby, K.; Cisneros-Zevallos, L.; Byrne, D. H. Comparison of ABTS, DPPH, FRAP, and ORAC assays for estimating antioxidant activity from guava fruit extracts. *Journal of food composition and analysis* 2006, 19, 669–675.
26. Bauer, A.; Kirby, W.; Sherris, J. C.; Turck, M. Antibiotic susceptibility testing by a standardized single disk method. *American journal of clinical pathology* 1966, 45, 493–496.
27. Andrews, J. M. The development of the BSAC standardized method of disc diffusion testing. *Journal of Antimicrobial Chemotherapy* 2001, 48, 29–42.
28. García-Barrasa, J.; López-de-Luzuriaga, J. M.; Monge, M. Silver nanoparticles: synthesis through chemical methods in solution and biomedical applications. *Central European journal of chemistry* 2011, 9, 7–19.
29. Walther, C. Comparison of colloid investigations by single particle analytical techniques—a case study on thorium-oxyhydroxides. *Colloids and Surfaces A: Physicochemical and Engineering Aspects* 2003, 217, 81–92.
30. Makarov, V.; Love, A.; Sinitsyna, O.; Makarova, S.; Yaminsky, I.; Taliansky, M.; Kalinina, N. “Green” nanotechnologies: synthesis of metal nanoparticles using plants. *Acta Naturae (англоязычная версия)* 2014, 6.
31. Jain, S.; Mehata, M. S. Medicinal plant leaf extract and pure flavonoid mediated green synthesis of silver nanoparticles and their enhanced antibacterial property. *Scientific Reports* 2017, 7, 15867.
32. Machado, R.; Alves-Pereira, I.; Ferreira, R. Plant growth, phytochemical accumulation and antioxidant activity of substrate-grown spinach. *Heliyon* 2018, 4, e00751.
33. Saravanakumar, A.; Ganesh, M.; Jayaprakash, J.; Jang, H. T. Biosynthesis of silver nanoparticles using *Cassia tora* leaf extract and its antioxidant and antibacterial activities. *Journal of Industrial and*

Engineering Chemistry 2015, 28, 277–281.

34. Bharathi, D.; Josebin, M. D.; Vasantharaj, S.; Bhuvaneshwari, V. Biosynthesis of silver nanoparticles using stem bark extracts of *Diospyros montana* and their antioxidant and antibacterial activities. *Journal of Nanostructure in Chemistry* 2018, 8, 83–92.
35. Khoshnamvand, M.; Huo, C.; Liu, J. Silver nanoparticles synthesized using *Allium ampeloprasum* L. leaf extract: Characterization and performance in catalytic reduction of 4-nitrophenol and antioxidant activity. *Journal of Molecular Structure* 2019, 1175, 90–96.
36. Machado, S.; Pinto, S.; Grosso, J.; Nouws, H.; Albergaria, J. T.; Delerue-Matos, C. Green production of zero-valent iron nanoparticles using tree leaf extracts. *Science of the Total Environment* 2013, 445, 1–8.
37. Helmlinger, J.; Sengstock, C.; Gross-Heitfeld, C.; Mayer, C.; Schildhauer, T.; Köller, M.; Epple, M. Silver nanoparticles with different size and shape: equal cytotoxicity, but different antibacterial effects. *RSC Advances* 2016, 6, 18490–18501.
38. Raza, M. A.; Kanwal, Z.; Rauf, A.; Sabri, A. N.; Riaz, S.; Naseem, S. Size- and shape-dependent antibacterial studies of silver nanoparticles synthesized by wet chemical routes. *Nanomaterials* 2016, 6, 74.
39. Pal, S.; Tak, Y. K.; Song, J. M. Does the antibacterial activity of silver nanoparticles depend on the shape of the nanoparticle? A study of the gram-negative bacterium *Escherichia coli*. *Applied and environmental microbiology* 2007, 73, 1712–1720.
40. Rout, A.; Jena, P. K.; Sahoo, D.; Bindhani, B. K. Green synthesis of silver nanoparticles of different shapes and its antibacterial activity against *Escherichia coli*. *Int. J. Curr. Microbiol. App. Sci* 2014, 3, 374–383.
41. Solidum, R. S.; Alguno, A. C.; Capangpangan, R. Controlling the Surface Plasmon Absorption of Silver Nanoparticles via Green Synthesis Using *Pennisetum purpureum* Leaf Extract. In *Key Engineering Materials*; Trans Tech Publ, 2018; pp 73–77.
42. Palem, R. R.; Ganesh, S. D.; Kroneková, Z.; Sláviková, M.; Saha, N.; Saha, P. Green synthesis of silver nanoparticles and biopolymer nanocomposites: a comparative study on physico-chemical, antimicrobial and anticancer activity. *Bulletin of Materials Science* 2018, 41, 55.
43. Hafez, R. A.; Abdel-Wahhab, M. A.; Sehab, A. F.; El-Din, A.-Z. A. K. Green synthesis of silver nanoparticles using *Morus nigra* leave extract and evaluation their antifungal potency on phytopathogenic fungi. *Journal of Applied Pharmaceutical Science Vol* 2017, 7, 041–048.
44. Keshari, A. K.; Srivastava, R.; Singh, P.; Yadav, V. B.; Nath, G. Antioxidant and antibacterial activity of silver nanoparticles synthesized by *Cestrum nocturnum*. *Journal of Ayurveda and integrative medicine* 2018.
45. Salehi, S.; Shandiz, S. A. S.; Ghanbar, F.; Darvish, M. R.; Ardestani, M. S.; Mirzaie, A.; Jafari, M. Phytosynthesis of silver nanoparticles using *Artemisia marschalliana* Sprengel aerial part extract and assessment of their antioxidant, anticancer, and antibacterial properties. *International journal of nanomedicine* 2016, 11, 1835.

46. Shaik, M. R.;Khan, M.;Kuniyil, M.;Al-Warthan, A.;Alkathlan, H. Z.;Siddiqui, M. R. H.;Shaik, J. P.;Ahamed, A.;Mahmood, A.; Khan, M. Plant-Extract-Assisted Green Synthesis of Silver Nanoparticles Using *Origanum vulgare* L. Extract and their Microbicidal Activities. *Sustainability* 2018, *10*, 913.
47. Khatami, M.;Noor, F. G.;Ahmadi, S.; Aflatoonian, M. Biosynthesis of Ag nanoparticles using *Salicornia bigelovii* and its antibacterial activity. *Electronic physician* 2018, *10*, 6733.
48. Chandirika, J. U.;Sindhu, R.;Selvakumar, S.; Annadurai, G. Herbal Extract Encapsulated in Chitosan Nanoparticle: a Novel Strategy for the Treatment of Urolithiasis. *indo american journal of pharmaceutical sciences* 2018, *5*, 1955–1961.
49. Haiss, W.;Thanh, N. T.;Aveyard, J.; Fernig, D. G. Determination of size and concentration of gold nanoparticles from UV – Vis spectra. *Analytical chemistry* 2007, *79*, 4215–4221.
50. Morones, J. R.;Elechiguerra, J. L.;Camacho, A.;Holt, K.;Kouri, J. B.;Ramírez, J. T.; Yacaman, M. J. The bactericidal effect of silver nanoparticles. *Nanotechnology* 2005, *16*, 2346.
51. Kim, K.-J.;Sung, W. S.;Suh, B. K.;Moon, S.-K.;Choi, J.-S.;Kim, J. G.; Lee, D. G. Antifungal activity and mode of action of silver nano-particles on *Candida albicans*. *Biometals* 2009, *22*, 235–242.
52. Panáček, A.;Kolář, M.;Večeřová, R.;Prucek, R.;Soukupová, J.;Kryštof, V.;Hamal, P.;Zbořil, R.; Kvítek, L. Antifungal activity of silver nanoparticles against *Candida* spp. *Biomaterials* 2009, *30*, 6333–6340.
53. Kvítek, L.;Panáček, A.;Soukupova, J.;Kolář, M.;Večeřová, R.;Prucek, R.;Holecova, M.; Zbořil, R. Effect of surfactants and polymers on stability and antibacterial activity of silver nanoparticles (NPs). *The Journal of Physical Chemistry C* 2008, *112*, 5825–5834.
54. Feng, Q. L.;Wu, J.;Chen, G.;Cui, F.;Kim, T.; Kim, J. A mechanistic study of the antibacterial effect of silver ions on *Escherichia coli* and *Staphylococcus aureus*. *Journal of biomedical materials research* 2000, *52*, 662–668.
55. Perumalla, A.; Hettiarachchy, N. S. Green tea and grape seed extracts—Potential applications in food safety and quality. *Food Research International* 2011, *44*, 827–839.
56. Korshed, P. The molecular mechanisms of the antimicrobial properties of laser processed nanoparticles. University of Manchester, 2018.
57. Umadevi, M.;Rani, T.;Balakrishnan, T.; Ramanibai, R. Antimicrobial activity of silver nanoparticles prepared under an ultrasonic field. *Int J Pharm Sci Nanotech* 2011, *4*, 1491–1496.
58. Mittal, A. K.;Chisti, Y.; Banerjee, U. C. Synthesis of metallic nanoparticles using plant extracts. *Biotechnology advances* 2013, *31*, 346–356.
59. Mourdikoudis, S.;Pallares, R. M.; THANH, N. T. K. Characterization Techniques for Nanoparticles: Comparison and Complementarity upon Studying Nanoparticle Properties. *Nanoscale* 2018.
60. Anandalakshmi, K.;Venugobal, J.; Ramasamy, V. Characterization of silver nanoparticles by green synthesis method using *Petalium murex* leaf extract and their antibacterial activity. *Applied Nanoscience* 2016, *6*, 399–408.
61. Prakash, P.;Gnanaprakasam, P.;Emmanuel, R.;Arokiyaraj, S.; Saravanan, M. Green synthesis of silver nanoparticles from leaf extract of *Mimusops elengi*, Linn. for enhanced antibacterial activity against

- multi drug resistant clinical isolates. *Colloids and Surfaces B: Biointerfaces* 2013, *108*, 255–259.
62. Shankar, S. S.; Ahmad, A.; Sastry, M. Geranium leaf assisted biosynthesis of silver nanoparticles. *Biotechnology progress* 2003, *19*, 1627–1631.
63. Chiguvare, H.; Oyedeji, O. O.; Matewu, R.; Aremu, O.; Oyemitan, I. A.; Oyedeji, A. O.; Nkeh-Chungag, B. N.; Songca, S. P.; Mohan, S.; Oluwafemi, O. S. Synthesis of Silver Nanoparticles Using Buchu Plant Extracts and Their Analgesic Properties. *Molecules* 2016, *21*, 774.
64. Jyoti, K.; Baunthiyal, M.; Singh, A. Characterization of silver nanoparticles synthesized using *Urtica dioica* Linn. leaves and their synergistic effects with antibiotics. *Journal of Radiation Research and Applied Sciences* 2016, *9*, 217–227.
65. Erjaee, H.; Rajaian, H.; Nazifi, S. Synthesis and characterization of novel silver nanoparticles using *Chamaemelum nobile* extract for antibacterial application. *Advances in Natural Sciences: Nanoscience and Nanotechnology* 2017, *8*, 025004.
66. Awwad, A. M.; Salem, N. M. Green Synthesis of Silver Nanoparticles by Mulberry Leaves Extract. *Nanoscience and Nanotechnology* 2012, *2*, 125–128.
67. Gudikandula, K.; Vadapally, P.; Charya, M. S. Biogenic synthesis of silver nanoparticles from white rot fungi: Their characterization and antibacterial studies. *OpenNano* 2017, *2*, 64–78.
68. Mohammed, A. E.; Al-Qahtani, A.; Al-Mutairi, A.; Al-Shamri, B.; Aabed, K. Antibacterial and Cytotoxic Potential of Biosynthesized Silver Nanoparticles by Some Plant Extracts. *Nanomaterials (Basel, Switzerland)* 2018, *8*.
69. Ajitha, B.; Reddy, Y. A. K.; Reddy, P. S. Biogenic nano-scale silver particles by *Tephrosia purpurea* leaf extract and their inborn antimicrobial activity. *Spectrochimica Acta Part A: Molecular and Biomolecular Spectroscopy* 2014, *121*, 164–172.
70. Ponarulsevam, S.; Panneerselvam, C.; Murugan, K.; Aarthi, N.; Kalimuthu, K.; Thangamani, S. Synthesis of silver nanoparticles using leaves of *Catharanthus roseus* Linn. G. Don and their antiplasmodial activities. *Asian Pacific Journal of Tropical Biomedicine* 2012, *2*, 574–580.
71. Al-Thabaiti, S. A.; Obaid, A. Y.; Hussain, S.; Khan, Z. Shape-directing role of cetyltrimethylammonium bromide on the morphology of extracellular synthesis of silver nanoparticles. *Arabian Journal of Chemistry* 2015, *8*, 538–544.
72. Veronesi, G.; Deniaud, A.; Gallon, T.; Jouneau, P.-H.; Villanova, J.; Delangle, P.; Carrière, M.; Kieffer, I.; Charbonnier, P.; Mintz, E. Visualization, quantification and coordination of Ag⁺ ions released from silver nanoparticles in hepatocytes. *Nanoscale* 2016, *8*, 17012–17021.
73. Burda, C.; Chen, X.; Narayanan, R.; El-Sayed, M. A. Chemistry and properties of nanocrystals of different shapes. *Chemical reviews* 2005, *105*, 1025–1102.

Figures

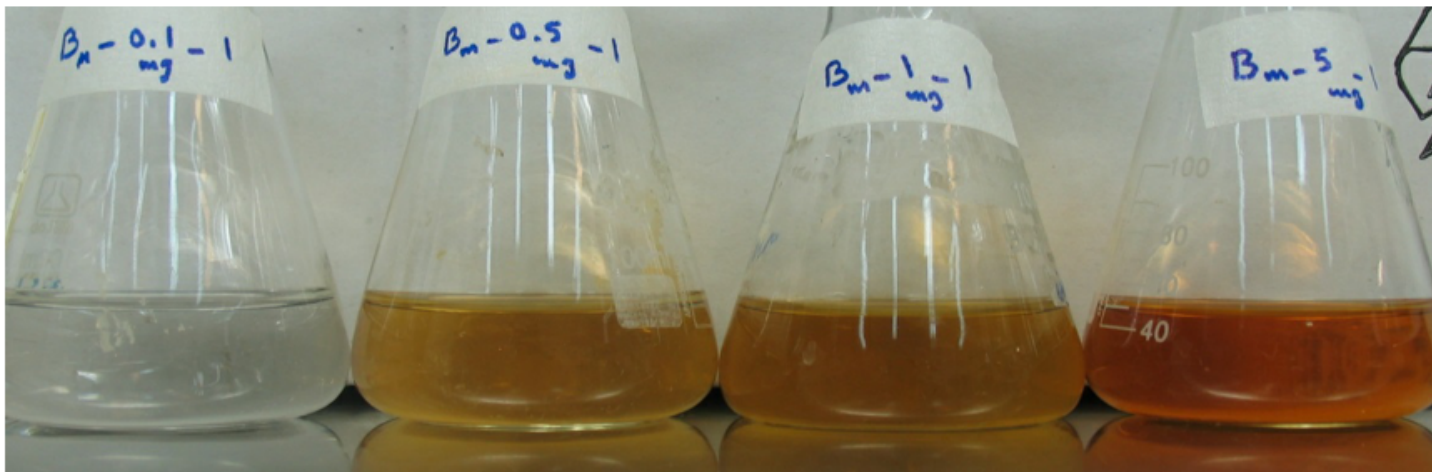


Figure 1

Left-to-right indicated color change in different volumes (7, 10, 15 and 20 ml) of aqueous extract of lemon balm after 30 minutes.

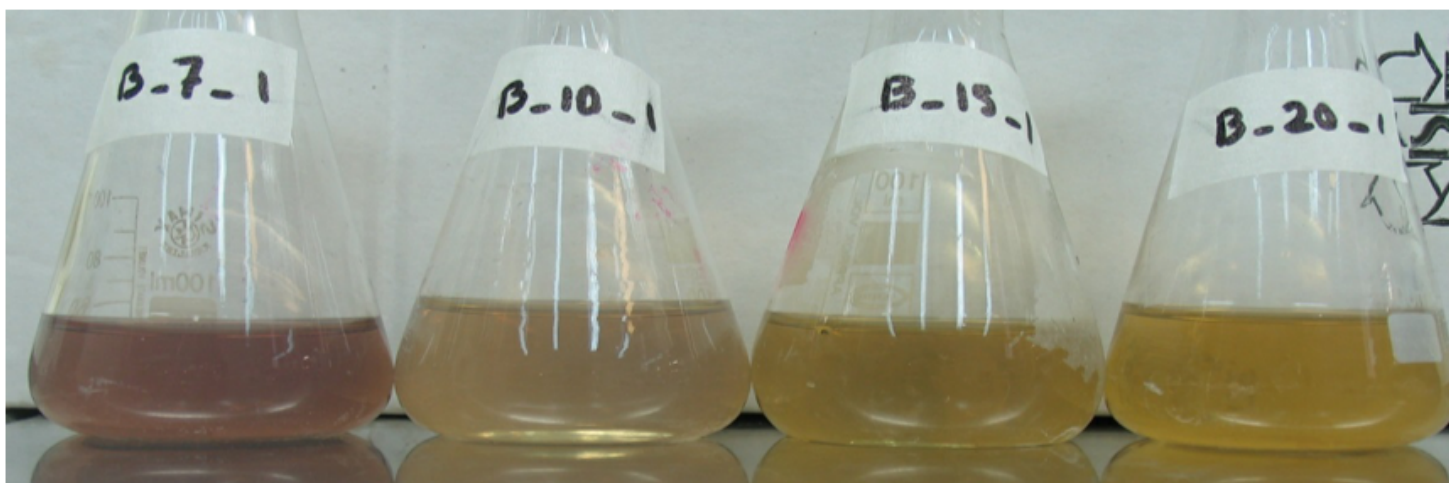


Figure 2

Left-to-right indicated color change in different concentrations (0.1, 0.5, 1, and 5 mg /50 ml) of methanolic extracts of lemon balm after 15 minutes.

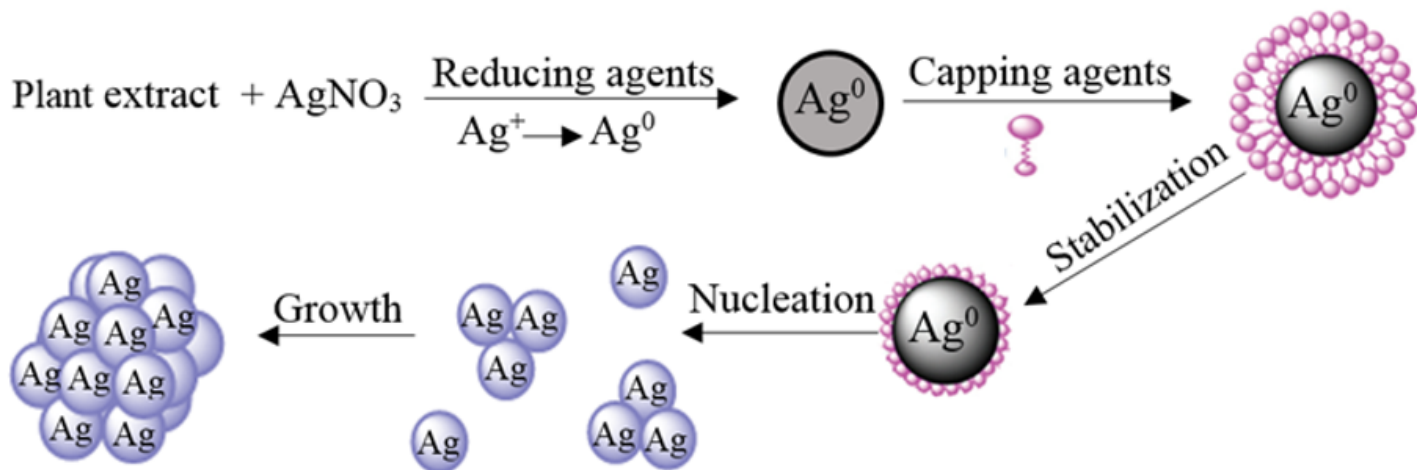


Figure 3

The reducing agents (in plant extract) donate electrons to Ag⁺ ions lead them as neutral Ag atoms (Ag⁰). These atoms due to van der waal's forces of attractions come closer and combine to form cluster of Ag atoms of diameter 1 to 100 nm, called Ag nanoparticle. A silver nanoparticle in nano scale may contain about hundreds atoms of silver. If these clusters (nanoparticles) come closer they agglomerate first and then aggregate to form bulky particles, which is not Ag nanoparticles. Plant extract has ability to stabilize silver colloids in water and prevent agglomeration and aggregation of the nanoparticles [28, 71-73].

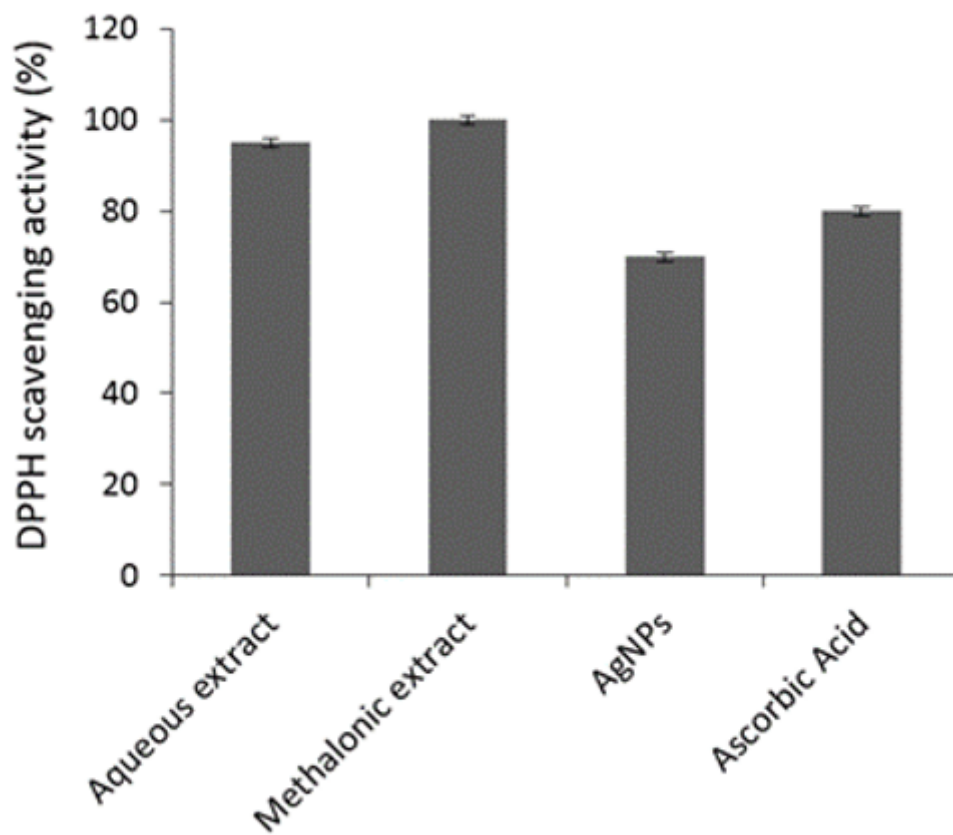


Figure 4

DPPH radical scavenging activity of two extracts of lemon balm and the synthesized AgNPs using methanolic extract. The methanolic extract had the highest antioxidant activity among the samples.

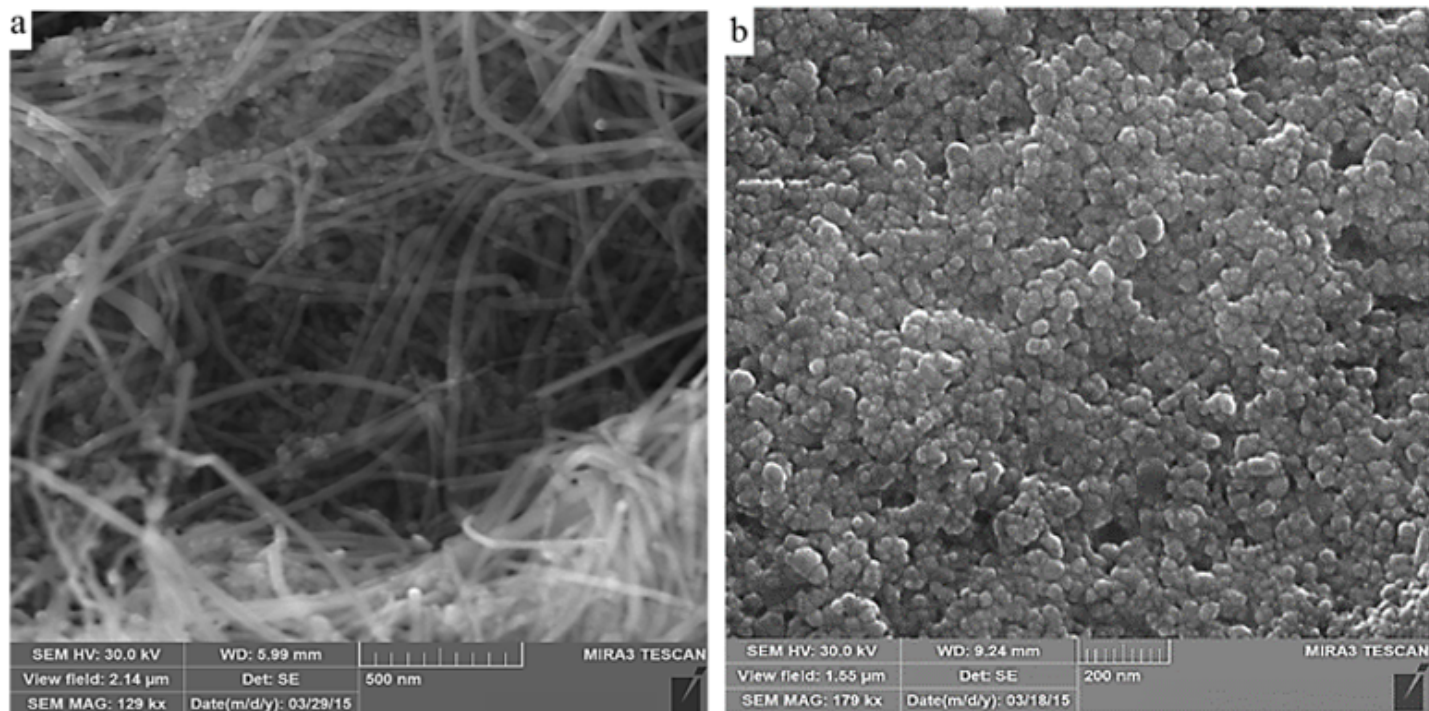


Figure 5

SEM images of biosynthesized silver nanoparticles by using different extracts of lemon balm; a) rod-shaped nanoparticles from aqueous extract and b) spherical shape nanoparticles from methanolic extract.

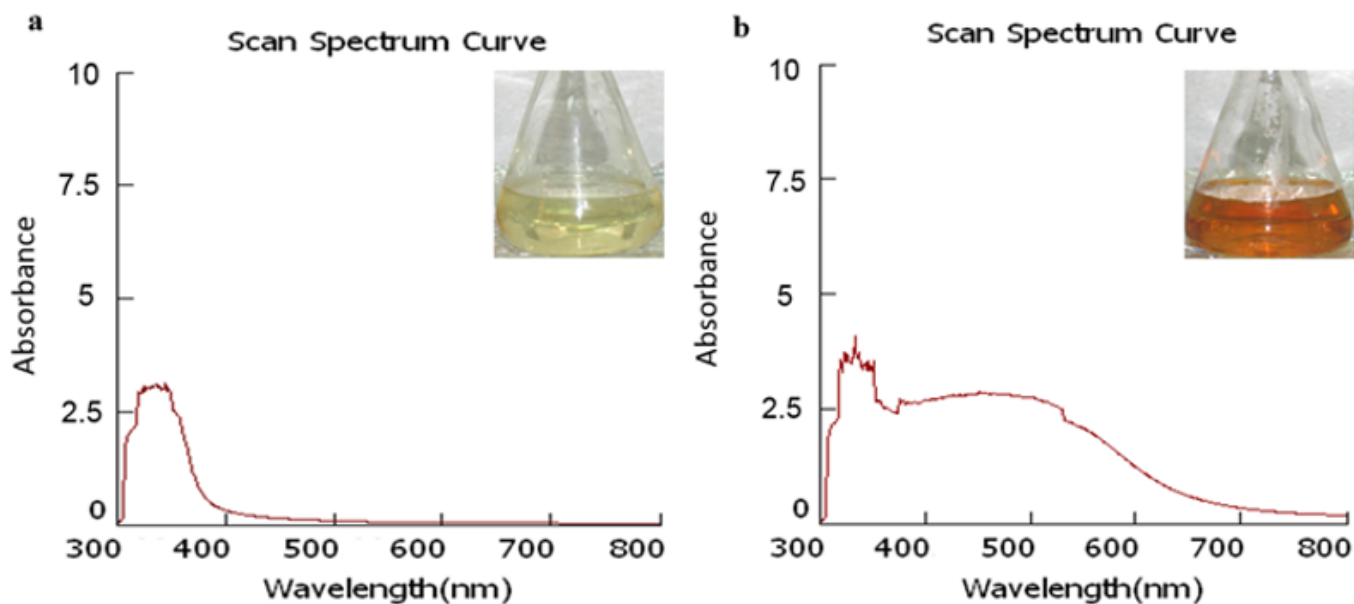


Figure 6

UV-Vis absorption spectrum of the photosynthesized AgNPs. a) The reaction at time zero showed no absorption in 400–500 nm region. b) Spectra represented the formation of silver nanoparticles with the help of lemon balm methanolic extract. The absorption of the SNPs was observed near 450 nm which is due to surface Plasmon resonance of AgNPs.

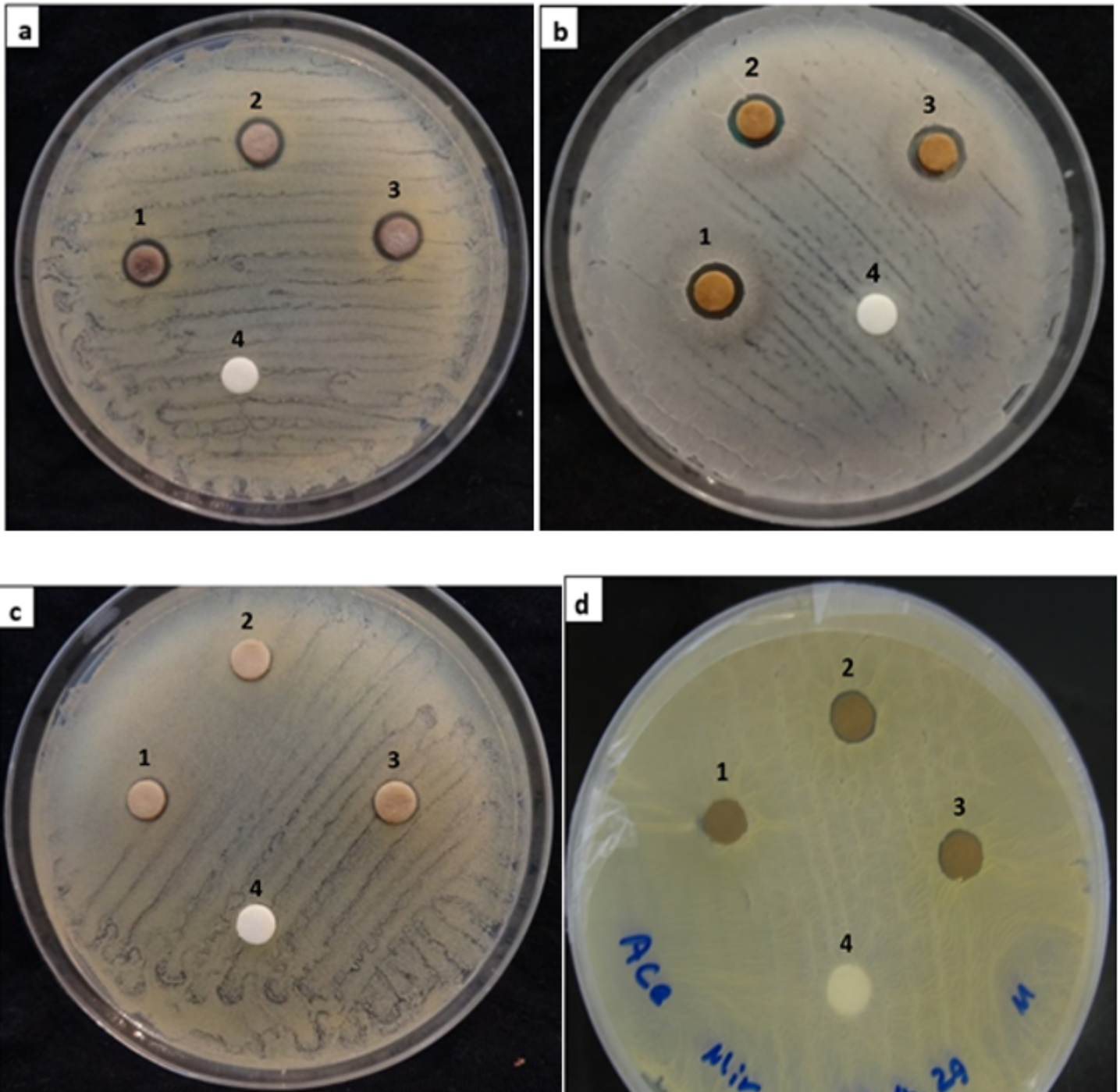


Figure 7

Inhibition zones produced by biosynthesized AgNPs at different volumes; 1) lemon balm methanolic extract, 2) 30 and 3) 40 μ l of biosynthesized nanoparticle solution plus 4) distilled water evaluated by disc diffusion method against a) *E. coli*, b) *S. aureus*, c) *B. subtilis* and d) *S. cerevisiae*.

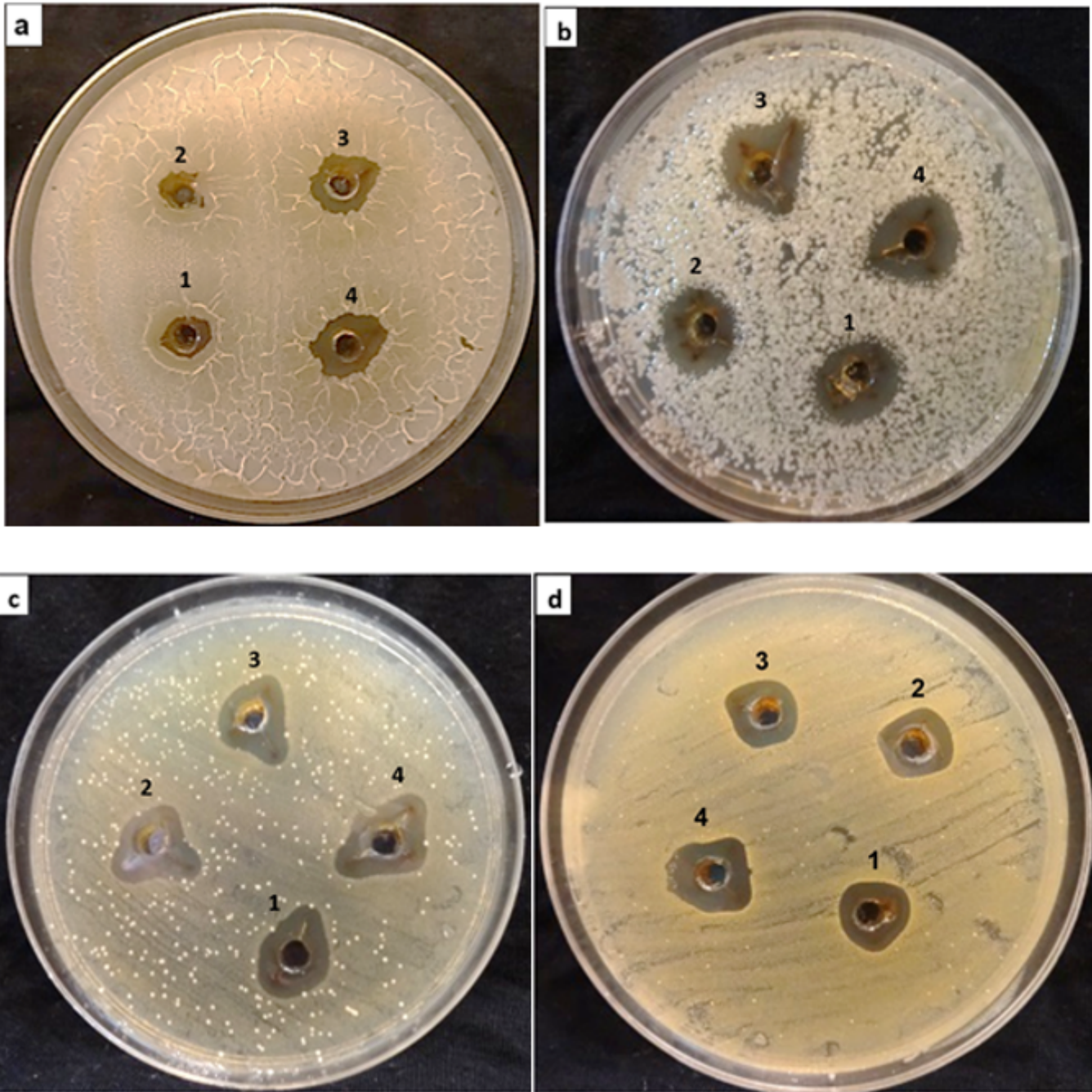


Figure 8

Antimicrobial activity of biosynthesized AgNPs at different volumes; 1) lemon balm methanolic extract, 2) 20, 3) 30 and 4) 40 μ l of biosynthesized nanoparticle solution evaluated by agar well diffusion method against a) *S. cerevisiae*, b) *B. subtilis*, c) *E. coli* and d) *S. aureus*.

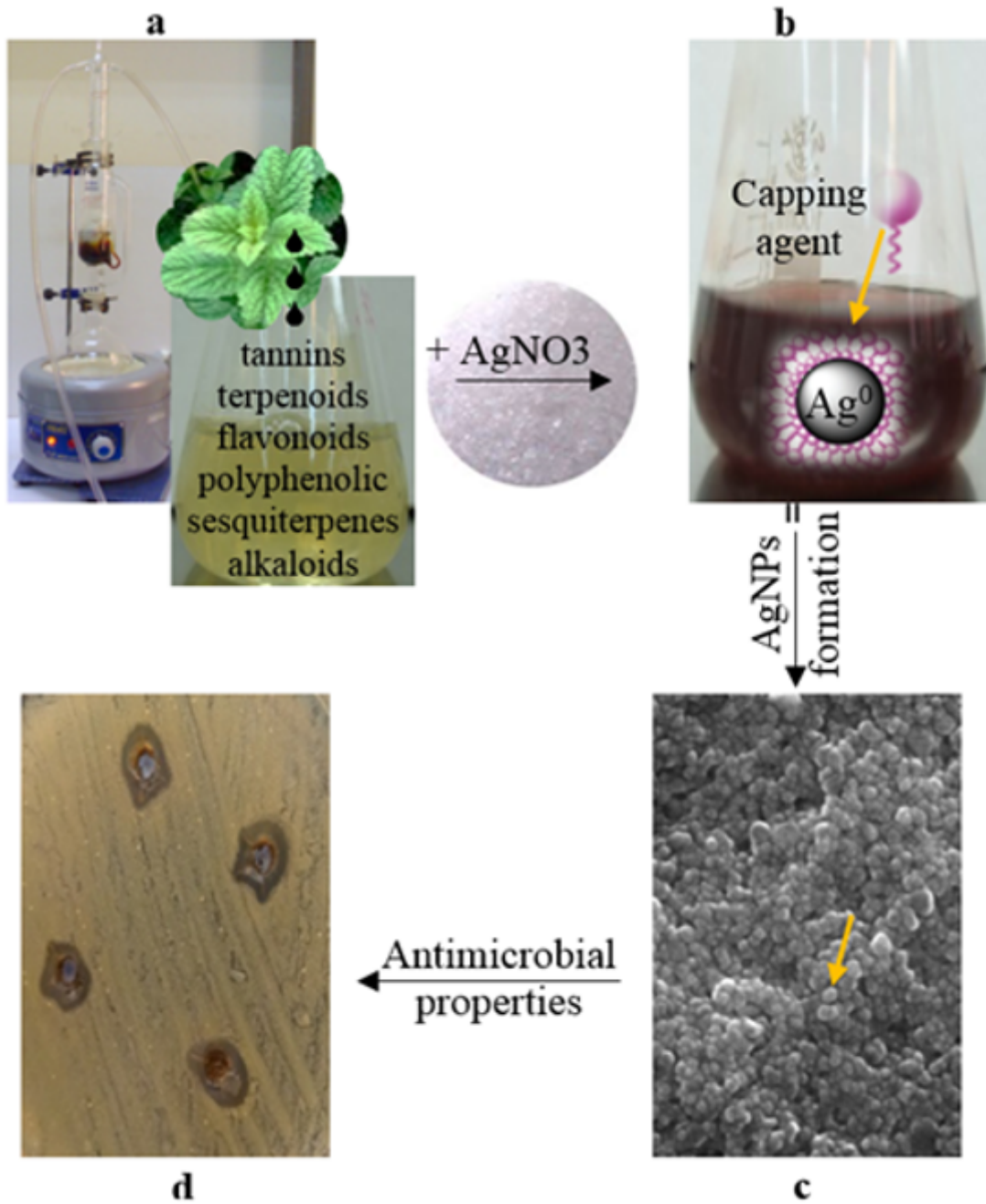


Figure 9

Proposed mechanism of AgNPs formation and antimicrobial activities exerted by *M. officinalis*. a) plant extract containing different organic compounds, b) *M. officinalis* extract acts as reducing and stabilizing agents, c) silver nanoparticles formation by the extract agents and d) antimicrobial activity of AgNPs.

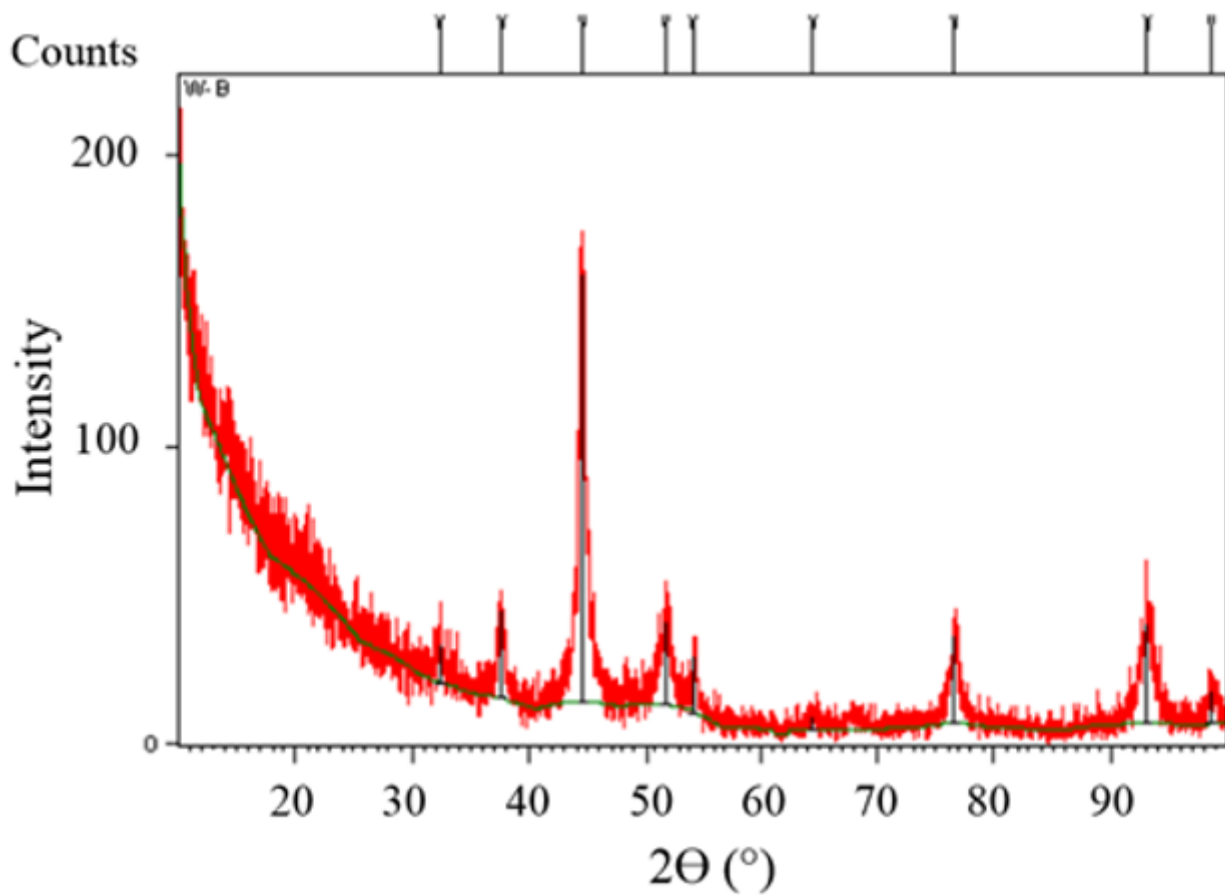


Figure 10

XRD diffractogram of biosynthesized AgNPs by *M. officinalis* methanolic extract.

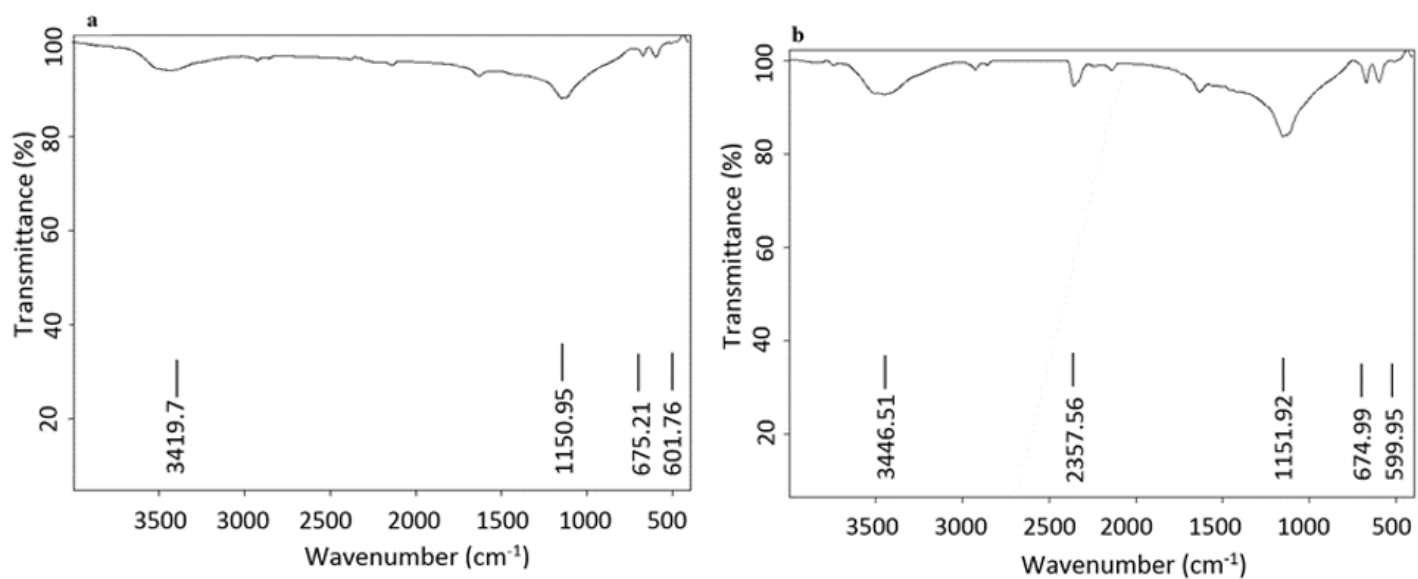


Figure 11

FTIR spectra of (a) *M. officinalis* methanolic extract and (b) biosynthesized AgNPs from *M. officinalis* methanolic extract.

Supplementary Files

This is a list of supplementary files associated with this preprint. Click to download.

- [graphicalabstarct.docx](#)